

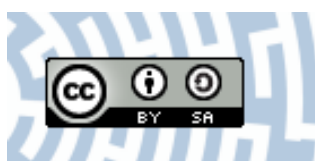


You have downloaded a document from
RE-BUS
repository of the University of Silesia in Katowice

Title: Electro-acoustic transducers on the basis of thin PZT-films

Author: Zygmunt Surowiak, Dionizy Czekaj, A. A. Bakirov, V. P. Dudkevich

Citation style: Surowiak Zygmunt, Czekaj Dionizy, Bakirov A. A., Dudkevich V. P. (1999). Electro-acoustic transducers on the basis of thin PZT-films. "Archives of Acoustics" (Vol. 24, no. 3 (1999) s. 379-390).



Uznanie autorstwa - Na tych samych warunkach - Licencja ta pozwala na kopiowanie, zmienianie, rozprowadzanie, przedstawianie i wykonywanie utworu tak długo, jak tylko na utwory zależne będzie udzielana taka sama licencja.



ELECTRO-ACOUSTIC TRANSDUCERS ON THE BASIS OF THIN PZT FILMS

Z. SUROWIAK, D. CZEKAJ

University of Silesia, Faculty of Engineering
Department of Materials Science
(41-200 Sosnowiec, 2, Śnieżna St., Poland)
e-mail:surowiak@us.edu.pl

A.A. BAKIROV and V.P. DUDKIEVICH

Rostov State University, Faculty of Physics
Department of Crystal Physics
(SU-344101 Rostov-on-Don, 194, Stachki Ave., Russia)

In the present work PZT-type thin films have been obtained by RF sputtering and electroacoustic transducers characterized by high sensitivity (γ), wide range of measured relative deformations (η) and high working frequencies (ω) were built. Polycrystalline ferroelectric thin films with the perovskite type structure and chemical composition $\text{Pb}(\text{Zr}_{0.53}\text{Ti}_{0.45}\text{W}_{0.01}\text{Cd}_{0.01})\text{O}_3$ have been fabricated by RF sputtering. The films exhibited slightly lower values of dielectric constant, residual polarization and piezoelectric coefficient $d_{33} = 80 \times 10^{-12}$ C/N, as compared with the ceramics of the same chemical composition. The thin films keep such a value of d_{33} up to the Curie point. On the basis of the PZT-type thin films the isotropic and anisotropic piezoelectric sensors were built and investigated. The electrical signal of the isotropic sensors is proportional to the sum of the main components of the relative deformation tensor whereas the signal of the anisotropic sensors depends on the angle ϕ between the sensor axis and the main axis of the deformation tensor of the sample under investigation. The sensors are characterized by high stability of the generated signal.

1. Introduction

There are several reasons for the increasing importance of ferroelectric thin films. Firstly, the trend toward miniaturisation of electronic components has led to the development of thin-film ferroelectric devices performing the same electronic functions, with only a fraction of the volume of devices based on bulk ceramics or single-crystal elements. Secondly, ferroelectric thin films are fast replacing expensive single crystal ferroelectrics. Thin films have the additional designing advantages of a small volume and a large geometrical flexibility over single crystals. Thirdly, new areas of application are being identified that utilise new device concepts, exploiting properties that are unique to both thin films and ferroelectric materials.

It is a common knowledge that for applications of ferroelectric thin films in electronics and optical devices, bulk ferroelectric properties must be achieved in thin films.

Therefore, a high-quality ferroelectric thin film should possess these properties: a stoichiometric composition, a dense and crystalline microstructure, a single-crystal or, at least, a preferentially oriented polycrystalline structure and uniformity over large areas.

Ferroelectric thin films of different chemical composition (e.g. BaTiO_3 , PbTiO_3 , $\text{Pb}(\text{Zr},\text{Ti})\text{O}_3$, $(\text{Pb},\text{La})(\text{Zr},\text{Ti})\text{O}_3$, KNbO_3 , LiNbO_3 , $(\text{Sr},\text{Ba})\text{TiO}_3$, $\text{Bi}_4\text{Ti}_3\text{O}_{12}$, and an organic polymer polyvinylidene fluoride) have been extensively studied for a wide variety of electrical and optical applications. Let us mention a few of them, namely: high dielectric capacitors [1, 2] and nonlinear capacitors [3], piezoelectric sensors of dynamical deformation [3–5], electroacoustic transducers [6], high-frequency surface acoustic wave (SAW) devices [7, 8], ultrasonic sensors [9], pyroelectric sensors and sensor arrays [3, 10–12], ferroelectric memory cells [13–17], optical waveguide devices or optical modulators [17], ferroelectric gates (FETs) [18], metal/insulator/semiconductor transistors (MIST) devices and many others [e.g. 19–22]. However, lead zirconate — titanate (PZT) — type thin films have received the most intensive study and will be emphasized in this article.

The reported methods to produce PZT films include, among others, various vapour-phase deposition techniques such as plasma and ion-beam sputter deposition, pulsed laser-ablation deposition, electron-beam or oven-induced evaporation for molecular-beam epitaxy, sol-gel process, metallorganic decomposition, and metallorganic chemical vapour deposition. However, additional research is still necessary to optimize the techniques to produce device-quality films on large semiconductor substrates in a way that is fully compatible with existing semiconductor process technology. Of all the reported techniques, the radio frequency (RF) sputtering technique appears to be promising because it offers the advantages of high deposition rates, film uniformity, composition control, high film densities and compatibility with integrated circuit technology [23, 24].

In the present work the lead-zirconate titanate (PZT)-type thin films have been obtained by RF sputtering. The sputtering parameters have been optimised in order to assure the composition transfer between the target and the film. Piezoelectric characteristics of the films were measured and electroacoustic transducers characterized by high sensitivity (γ), wide range of measured relative deformations (η) and high working frequencies (ω) were built.

2. Technology of the thin film preparation

The thin PZT films were obtained by RF sputtering. Two sputtering systems were used for the thin film preparation. A system I made it possible to sputter powdered target obtained from crushed ceramics of the chemical composition $\text{Pb}(\text{Zr}_{0.53}\text{Ti}_{0.45}\text{W}_{0.01}\text{Cd}_{0.01})\text{O}_3$. The coarse-grained powder was placed in the quartz vessel of 0.1 m in diameter and 5 mm high and covered the bottom of the vessel with a 2–5 mm thick layer. The RF generator was operating in the continuous mode during deposition.

A system II made it possible to sputter a disk target of $\text{Pb}(\text{Zr}_{0.53}\text{Ti}_{0.45}\text{W}_{0.01}\text{Cd}_{0.01})\text{O}_3$ ceramics obtained by hot pressing. Water-cooling of the cathode and the pulse operation mode of the RF generator avoid overheating of the target during sputtering.

Table 1. Technological conditions of the thin film preparation.

	SYSTEM I	SYSTEM II
material	coarse-grained powder of $\text{Pb}(\text{Zr}_{0.53}\text{Ti}_{0.45}\text{W}_{0.01}\text{Cd}_{0.01})\text{O}_3$ ceramics; 0.15 - 0.40 mm	hot-pressed disk target of $\text{Pb}(\text{Zr}_{0.53}\text{Ti}_{0.45}\text{W}_{0.01}\text{Cd}_{0.01})\text{O}_3$
heating	electron-ion bombardment; $T_s = 600 - 1073 \text{ K}$	resistance heater $T_s = 600 - 1073 \text{ K}$
generator	continuous mode of operation: $f = 13.6 \text{ MHz}$; $U_a = 5 \text{ kV}$; $i_a = 0.8 \text{ A}$; $N = 2.5 \text{ kW}$	pulse mode of operation: pulse duration $\tau = 0.1 - 1.2 \text{ ms}$; pulse period to pulse length ratio $\gamma = 2 - 7$
working gas	oxygen; $p = 30 - 80 \text{ Pa}$	oxygen; $p = 20 - 180 \text{ Pa}$
substrates	metal foils and dielectric plates $20 \times 30 \times 0.1 \text{ mm}^3$	platinum, stainless steel, monocrystalline mica, polycor
substrate-to-target distance	8 - 16 mm	8 - 16 mm

More detailed technological conditions used for the thin film preparation are presented in Table 1.

3. Chemical composition

Homogeneity check and investigation of the thin film composition have been performed by X-ray micro-probe analysis. The results are shown in Fig. 1 [25].

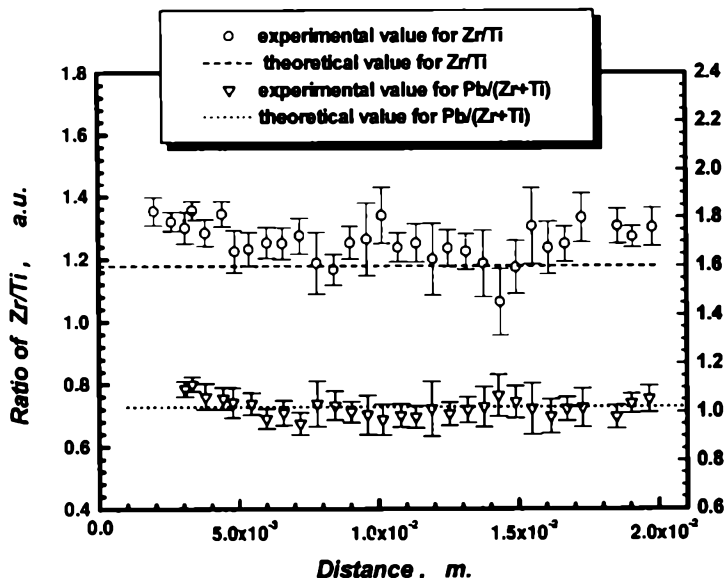


Fig. 1. Results of the analysis of homogeneity of the chemical composition of the PZT-type thin film (a probe was moved along a straight line parallel to an edge of the film): 1 - Zr/Ti; 2 - Pb/(Zr + Ti). Stoichiometric ratios of suitable components in the target are marked by dashed lines.

The stoichiometric ratio of the metallic components in the target is shown by dotted lines. As an indication of the measuring error the maximal deviations from the average value of 10 measurements are marked in the figure. As can be seen from Fig. 1 the thin PZT films obtained under optimal technological conditions are characterized by high homogeneity of the chemical composition and stoichiometry close to that of the target.

4. Piezoelectric characteristics

To obtain a piezoelectric effect one has to polarize thin films in an external electric field. The most stable polarization state was achieved by polarising them with the following conditions: sawtooth voltage with $E = 8 \times 10^7$ V/m, pulse arising time $t_1 = 5$ s, pulse decreasing time $t_2 = 5$ s and filling factor $k = 2$ (k is a ratio of the pulse period to pulse duration) was applied to the samples; at the same time the samples were heated to $T = 573$ K (in $t = 20$ minutes) and then cooled to room temperature in the same time so the total time of heat treatment was 40 min.

Piezoelectric properties are often described in terms of piezoelectric charge coefficients. The piezoelectric coefficient d_{ijk} is a third-rank tensor that relates a strain of a piezoelectric ceramic sample to an externally applied electric field. A contracted notation is often used so that tensor components may be written more easily. In the present study, the component d_{33} of the piezoelectric coefficient of the thin film was measured by a quasi-static method described in detail elsewhere [26].

Figure 2 shows the dependence of the piezoelectric coefficient d_{33} on the voltage U_0 which changes linearly with time at a rate of ± 0.003 V/s. A change of sign of piezoelectric coefficient from “+” to “-” was assumed conventionally (the change of sign of d_{33} is given by the change of direction of thin film polarization caused by the voltage $\pm U$).

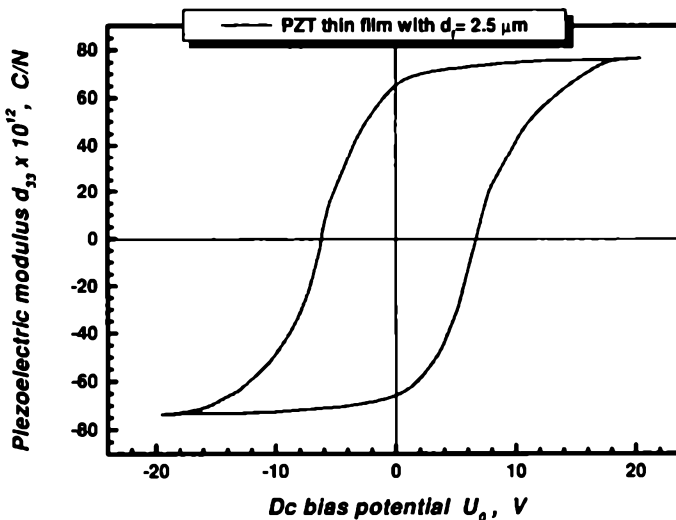


Fig. 2. Dependence of the piezoelectric coefficient d_{33} on the voltage U_0 for a PZT-type thin film with a thickness of $2.5 \mu\text{m}$.

It has been stated that the d_{33} value changes with the thickness of the film and that the saturation of the dependence is achieved for the thin film thickness of about 2.5 – 3.0 μm at the level of $d_{33} = 80 \times 10^{-12} \text{ C/N}$ ("thin" transition layer films, stainless-steel substrates: the films were polarized under the same conditions), whereas for the 5 – 6 μm thick PZT films the saturation is achieved at the level of $d_{33} = 25 - 30 \times 10^{-12} \text{ C/N}$ ("thick" transition layer; measuring field $E_0 = 25 \times 10^6 \text{ V/m}$). To illustrate the above mentioned effects the thickness dependencies of the component d_{33} of the piezoelectric coefficient are shown in Fig. 3.

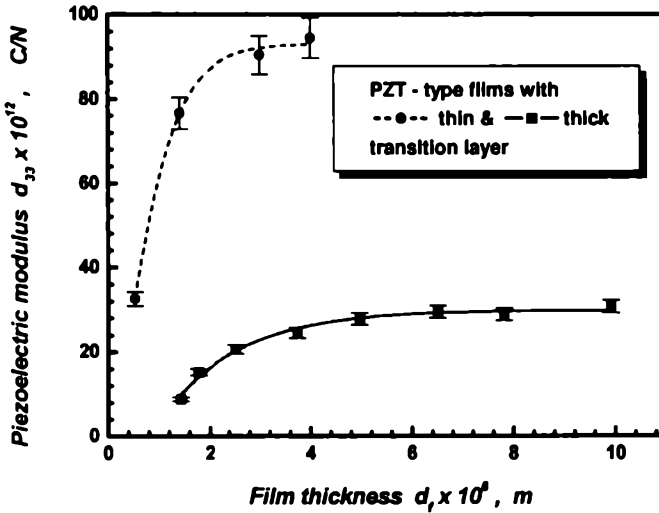


Fig. 3. Dependence of the piezoelectric coefficient d_{33} of the $\text{Pb}(\text{Zr}_{0.53}\text{Ti}_{0.45}\text{W}_{0.01}\text{Cd}_{0.01})\text{O}_3$ thin films with "thin" (dashed curve) and "thick" (solid curve) transition layer on thickness. All the films were polarized under the same conditions.

The temperature dependence of the piezoelectric coefficient d_{33} is shown in Fig. 4 and Fig. 5.

Figure 4 shows the temperature dependence of the piezoelectric coefficient d_{33} for the $\text{Pb}(\text{Zr}_{0.53}\text{Ti}_{0.45}\text{W}_{0.01}\text{Cd}_{0.01})\text{O}_3$ thin films with different microdeformations $\langle \Delta d/d \rangle$. In this connection, it should be noted that the mean microdeformation (strain) in the direction normal to the substrate $\langle \Delta d/d \rangle$ is the mean of the relative changes in interplanar distances d inside the crystallites (Δd — the absolute change in interplanar distances d). The value of mean strains depends on the field of mechanical stresses arising in the vicinity of chaotically distributed linear defects in structure and on the field of mechanical stresses arising in the vicinity of interblock and grain boundaries. It is usually taken as the measure of structural perfection of the films [27].

One can see from Fig. 4 that in the case of a relatively small deformation there is a diffused maximum at 433 K on the $d_{33}(T)$ curve, whereas in the case of a relatively large microdeformation there is no such a maximum and d_{33} does not significantly change with temperature up to about 513 K.

From the point of view of the temperature stability of the electro-acoustic transducers it is better to use thin films of the second type for fabrication of such transducers.

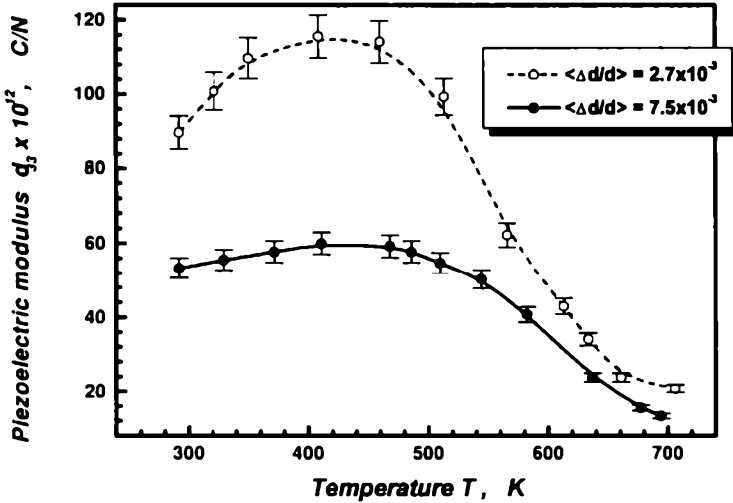


Fig. 4. Dependence of the piezoelectric coefficient d_{33} of the $\text{Pb}(\text{Zr}_{0.53}\text{Ti}_{0.45}\text{W}_{0.01}\text{Cd}_{0.01})\text{O}_3$ thin films versus temperature for films with different microdeformations $\langle \Delta d/d \rangle$.

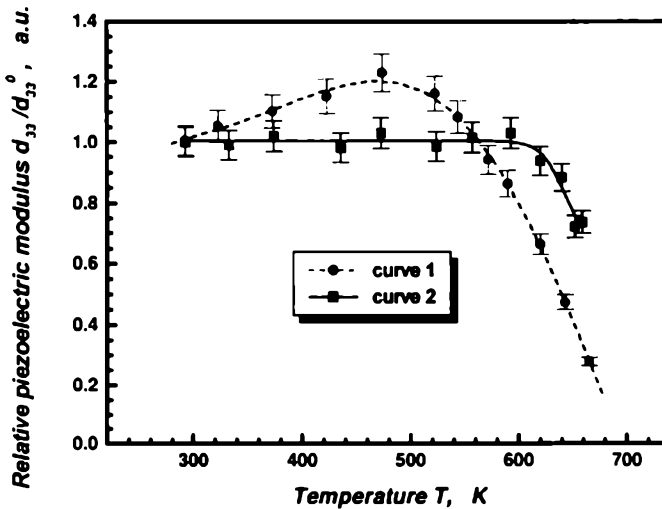


Fig. 5. Dependence of the piezoelectric coefficient d_{33} of PZT-type thin films with a thickness of $2.5 \mu\text{m}$ on temperature (curve 1) and dependence of d_{33} on temperature of primary heat treatment for measurements carried out at room temperature (curve 2).

However, it is worth noting that the thin films exhibit greater temperature stability of the piezoelectric coefficient than PZT ceramics do. This can be seen in Fig. 5 (curve 1). The $d_{33}(T)$ curve has a slight slope and there is no sharp peak near T_C (which appears for samples of ceramics). The increase in d_{33} with increasing T ends at a temperature $T \approx 593 \text{ K}$. This is related to changes in $\varepsilon(T)$ and $P_S(T)$: the dielectric permittivity consistently increases in value while the spontaneous polarization consistently decreases

when temperature increases. Both effects are characteristic for ferroelectrics with a diffuse phase transition. Curve 2 in Fig. 5 shows the temperature stability of the thin film polarization state when the action time of the raised temperature is short. This curve was obtained as follows: the polarized sample was first heated to the designated temperature and kept at that temperature for 5 minutes and then cooled to room temperature; after that heat treatment the d_{33} was measured. It is worth noting, that rather a strong piezoelectric activity exists even after heating the sample to the Curie point.

5. Thin film sensor fabrication and characteristics

To build isotropic deformation sensors, the thin PZT-film of about $2.0\text{--}2.5\mu\text{m}$ in thickness was deposited on stainless steel substrates. Disk-type aluminium electrodes were deposited on the upper side of the thin film by vacuum evaporation. These structures were cut into elements with the Al-electrode in the very centre. The thin film capacitors obtained (Fig. 6) were poled under experimentally chosen conditions.

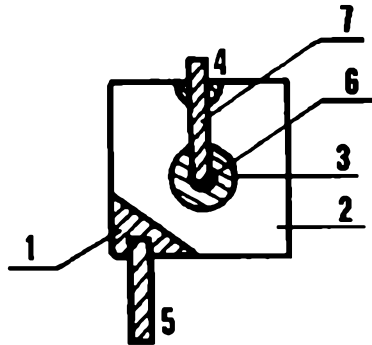


Fig. 6. Thin film isotropic sensor of dynamical deformation: diagram of sensor construction: 1 - substrate; 2 - upper surface of thin PZT film (not shaded); 3 - upper electrode; 7, 5 - electrical conductors welded on upper electrode (7) and substrate (5); 6 - silver drop or mark of point weld; 4 - electrical insulation of conductor (7) from substrate edge (1).

To obtain anisotropic deformation sensors, the PZT thin film was deposited on ceramic substrates (e.g. polycor). Planar interdigital Al-electrodes were deposited by photolithography on the upper side of the film. The dielectric gap width was equal to the width of a single "finger" of the electrode and was $12\mu\text{m}$, the length was $5\mu\text{m}$ and the total number of "fingers" was 200 (Fig. 7).

In Fig. 8 the dependence of the piezoelectric signal V of the isotropic sensor on the value of the sum of the deformation tensor main components $\eta(1 - \nu)$, where ν is the Poisson ration for steel ($\nu \approx 0.3$) and η is the relative deformation of the surface under investigations is presented [4]. One can see that the dependence is a linear one within the range of the investigated deformation. The lower limit of recorded relative deformation $\eta_{\min} = 10^{-9}$ is conditioned by the influence of acoustic noise, which can cause out-of-control deformation of the beam surface layer of $\gamma = 0.5 \times 10^{-10}$ order of magnitude. The upper limit of the recorded deformation $\eta_{\max} = 10^{-10}$ corresponds to

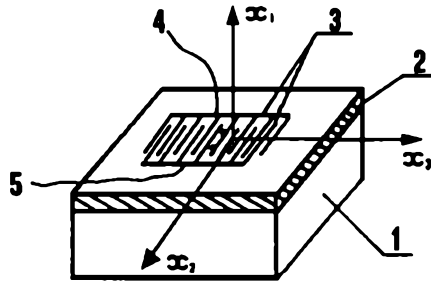


Fig. 7. Anisotropic sensor of dynamical deformation: 1 - polycrystalline substrate; 2 - thin ferroelectric film; 3 - planar comb-shaped electrodes; 4, 5 - electrical conductors. The arrows show the directions of polarization in the dielectric gaps.

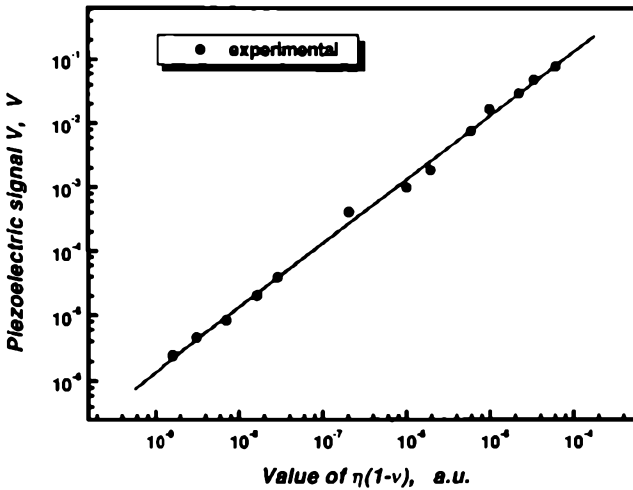


Fig. 8. Dependence of the piezoelectric signal V of isotropic sensor on the value of the sum of the deformation tensor main components $\eta(1 - \nu)$.

the plastic deformation threshold of the beam material. The basic parameters of the isotropic ferroelectric thin film deformation sensors are presented in Table 2. The values of the particular parameters have been obtained by complex investigations of many sensors under both laboratory and industrial conditions.

Taking into account the assumptions we used in describing the isotropic deformation sensor [4] as well as considering the deformation of the thin film in the direction normal to the substrate surface, one can show that the intensity E_3 of the electric field in the sensor (along the X_3 axis) is:

$$E_3 = h_{31} \left[- \left(\frac{s_{12}s_{33} - s_{13}^2}{s_{11}s_{33} - s_{13}^2} + 1 \right) (\eta'_2 \cos^2 \phi + \eta'_3 \sin^2 \phi) - \frac{s_{13}(s_{11} - s_{12})}{s_{11}s_{33} - s_{13}^2} (\eta'_2 \sin^2 \phi + \eta'_3 \cos^2 \phi) \right] - h_{33} (\eta'_2 \sin^2 \phi + \eta'_3 \cos^2 \phi), \quad (1)$$

Table 2. Sensor parameters.

1. Sensitivity	$\eta, V \dots\dots\dots 10^3$
	$\mu, C \dots\dots\dots 10^{-6}$
2. Range of deformation	$\Delta l/l, \dots\dots\dots 10^{-9} - 10^{-4}$
3. Range of frequency	Hz, $\dots\dots\dots 10^{-3} - 10^7$
4. Range of temperature	K, $\dots\dots\dots 77 - 573$
5. Electric capacitance	pF, $\dots\dots\dots 1000$
6. Dimensions of an active element	mm ³ , $\dots\dots\dots 2 \times 3 \times 0.1$
7. Mass	g, $\dots\dots\dots \leq 0.01$
8. Impact strength	m/s ² , $\dots\dots\dots 10^6$
9. No time lag	

where s_{ij} are the elements of the mechanical compliance matrix, h_{ij} are the elements of the piezoelectric coefficient matrix, ϕ is the angle between the axis of the sensor (direction of the thin film polarization in dielectric gaps) and the main axis of the deformation tensor of the sample under investigation, η is the relative deformation in the superficial beam layer, and η'_{ij} are the relative deformation tensor components.

For estimation of E_3 according to Eq. (1) the piezoelectric constants (h_{31} and h_{33}) and elements of the mechanical flexibility tensor ($s_{11}, s_{12}, s_{13}, s_{33}$) for polarized PZT-type ceramics of the same chemical composition were taken [22, 28] together with the following values of the other parameters: $\eta'_2 = -\nu\eta$, $\eta'_3 = \eta$, $\nu = 0.3$ and $\eta = 5 \times 10^{-6}$. To compare with the PZT-type sensor the calculations were also performed for polarized BaTiO₃ ceramics and for monocrystals of LiNbO₃. The s_{ij} - and h_{ij} -parameters are summarised in Table 3. The results of the calculations are shown in Fig. 9.

Table 3. Piezoelectric and mechanical constants chosen for calculations.

Quantity	PZT (ceramics)	BaTiO ₃ (ceramics)	LiNbO ₃ (monocrystal)
$h_{31}, V/m$	-0.78×10^9	0.35×10^9	0.55×10^9
$h_{33}, V/m$	4.58×10^9	1.48×10^9	5.90×10^9
$S_{33}^D, m^2/N$	7.50×10^{-12}	6.73×10^{-12}	4.67×10^{-12}
$S_{11}^D, m^2/N$	10.40×10^{-12}	8.18×10^{-12}	5.15×10^{-12}
$S_{13}^D, m^2/N$	-2.40×10^{-12}	-1.95×10^{-12}	-1.28×10^{-12}
$S_{12}^D, m^2/N$	-4.70×10^{-12}	-2.98×10^{-12}	-0.53×10^{-12}

It is evident from both theoretical calculations and the experimental data given in Fig. 9 that: i) there is an angle $\phi = \phi_0$ for which there is no piezoelectric signal ($E_3(\phi_0) = 0$); ii) the intensity of the electric field E_3 for the LiNbO₃ sensor is greater than the BaTiO₃ sensor signal; the angle $\phi_0 = 64.53^\circ$ for the LiNbO₃ sensor is greater than the angle $\phi_0 = 58.51^\circ$ for the PZT sensor and $\phi_0 = 57.66^\circ$ for the BaTiO₃ sensor; iii) experimental and theoretical values of E_3 differ considerably ($E_3 \text{ exp.} \geq 70\% E_3 \text{ theor.}$) whereas experimental and theoretical values of ϕ_0 are fairly similar ($\phi_0 \text{ exp.} \geq 95\% \phi_0 \text{ theor.}$).

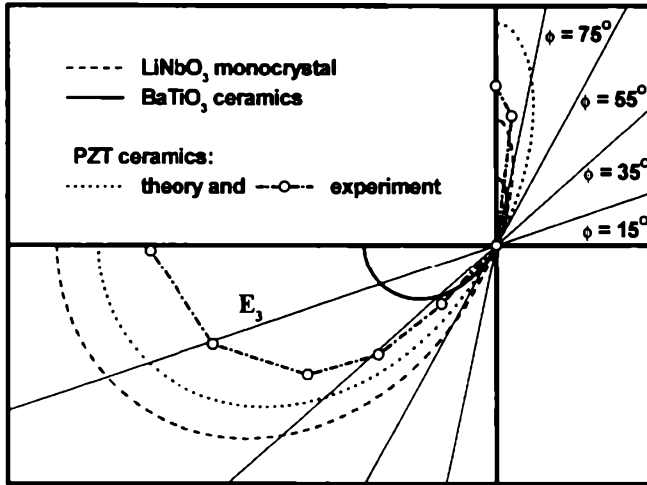


Fig. 9. Dependence of the anisotropic sensor signal E_3 on the angle ϕ between its axis and the main axis of the sample deformation tensor for LiNbO₃, BaTiO₃ and PZT-based sensors. The change in sign of E_3 should be interpreted as the change in polarity of the piezoelectric signal.

6. Conclusions

Polycrystalline ferroelectric thin films with the perovskite type structure and chemical composition $\text{Pb}(\text{Zr}_{0.53}\text{Ti}_{0.45}\text{W}_{0.01}\text{Cd}_{0.01})\text{O}_3$ have been fabricated by RF sputtering. The films exhibited slightly lower values of dielectric constant, residual polarization and piezoelectric coefficient $d_{33} = 80 \times 10^{-12} \text{ C/N}$, compared with ceramics of the same chemical composition. The thin films keep such a value of d_{33} up to the Curie point.

On the basis of the PZT-type thin films, isotropic and anisotropic piezoelectric sensors were built and investigated. The electrical signal of the isotropic sensors is proportional to the sum of the main components of the relative deformation tensor whereas the signal of the anisotropic sensors depends on the angle ϕ between the sensor axis and the main axis of the deformation tensor of the sample under investigation. The sensors are characterized by high stability of the generated signal.

Acknowledgements

The authors would like to thank the Committee for Scientific Research (KBN), Poland, for financial support under grant No. 7T08D 005 17.

References

- [1] K. OKAMOTO, Y. NASU and Y. HAMAKAWA, *Low-threshold-voltage thin-film electroluminescent devices*, IEEE Trans. Elec. Dev., **ED-28**, 6, 698-702 (1981).

- [2] R. KHAMANKAR, J. KIM, B. JIANG, C. SUDHAMA, P. MANIAR, R. MOAZZAMI, R. JONES and J. LEE, *Impact of post processing damages on performance of high dielectric constant PLZT thin film capacitors for ULSI DRAM applications*, International Electron Devices Meeting, San Francisco, CA, December 11-14, 1994, IEDM Technical Digest, 337-340 (1994).
- [3] R. WASER, *Recent trends in electroceramic thin films. Capacitors, pyroelectric sensors and piezoelectric devices*, [in:] *Electroceramics V International Conference on Electronic Ceramics and Applications*, J.L. BAPTISTA, J.A. LABRINCHA, P.M. VILARINHO [Eds.], University of Aveiro, Portugal 1996, 293-297.
- [4] Z. SUROWIAK, D. CZEKAJ, A.A. BAKIROV and V.P. DUDKEVICH, *Dynamical deformation sensors based on thin ferroelectric PZT films*, *Thin Solid Films*, **256**, 226-233 (1995).
- [5] D. CZEKAJ, Z. SUROWIAK, A.A. BAKIROV and V.P. DUDKEVICH, *Piezoelectric sensors of mechanical strains on the basis of the thin LiNbO₃ and BaTiO₃* [in Polish], *Akustyka Molekularna i Kwantowa*, **15**, 43-57 (1994).
- [6] N.F. FOSTER, *The deposition and piezoelectric characteristics of sputtered lithium niobate films*, *J. Appl. Phys.*, **40**, 1, 420-423 (1969).
- [7] J. DUDEK, *Piezoelectric acoustotransducers SAW on the basis of Pb(Zr,Ti)O₃*, The 8-th Piezoelectric Conference PIEZO'94, 5-7 October 1994, Zakopane, Poland, Proceedings, Tele & Radio Research Institute, 359-364 (1995).
- [8] H. ADACHI, T. MITSUYA, O. YAMAZAKI and K. WASA, *Ferroelectric (Pb,La)(Zr,Ti)O₃ epitaxial thin films on sapphire grown by RF-magnetron sputtering*, *J. Appl. Phys.*, **60**, 736-741 (1986).
- [9] Z. SUROWIAK and V.P. DUDKEVICH, *Thin ferroelectric films* [in Polish], Wyd. Univ. Śl., Katowice 1996, p.331.
- [10] P. MURALT, *PZT thin films for sensors and actuators*, [in:] *Electroceramics V, International Conference on Electronic Ceramics and Applications*, J.L. BAPTISTA, J.A. LABRINCHA, P.M. VILARINHO [Eds.], University of Aveiro, Portugal 1996, 11-18.
- [11] B. WILLENG, M. KOHLI, K. BROOKS, P. MURALT and N. SETTER, *Pyroelectric thin film sensor arrays integrated on silicon*, *Ferroelectrics*, **201**, 147-156 (1997).
- [12] J. KULEK, J.L. CHARTIER, R. LEBIHAN, L.M. HAFID and B. HILCZER, *Pyroelectric response and thermally stimulated current of PZT thin films*, *Ferroelectric Letters*, **22**, 83-88 (1997).
- [13] D. BONDURANT and F. GNADINGER, *Ferroelectrics for nonvolatile RAMs*, *IEEE Spectrum*, **7**, 30-33 (1989).
- [14] J.F. SCOTT and C.A. PAZ DE ARAUJO, *Ferroelectric memories*, *Science*, **246**, 1400-1405 (1989).
- [15] J.F. SCOTT, *Ferroelectric memories*, *Physics World*, **2**, 46-50 (1995).
- [16] A.C. PAZ DE ARAUJO, L.D. McMILLAN, B.M. MELNIK and J.D. CUCHIARO, *Ferroelectric memories*, *Integrated Ferroelectrics*, **104**, 241-256 (1990).
- [17] A.I. KINGON and S.K. STREIFFER, *Recent trends in electroceramic thin films: II. DRAMS, non-volatile memories, and optical devices*, [in:] *Electroceramics V, International Conference on Electronic Ceramics and Applications*, J.L. BAPTISTA, J.A. LABRINCHA, P.M. VILARINHO [Eds.], University of Aveiro, Portugal 1996, 299-303.
- [18] T. NAKAMURA, Y. NAKAO, A. KAMISAWA and H. TAKASU, *Ferroelectric memory FET with Ir/IrO₂ electrodes*, *Integrated Ferroelectrics*, **9**, 179-187 (1995).
- [19] K.R. UDAYAKUMAR, J. CHEN, A.M. FLYNN, S.F. BART, L.S. TAVROV, D.J. EHRlich, L.E. CROSS and R.A. BROOKS, *Ferroelectric thin films for piezoelectric micromotors*, *Ferroelectrics*, **160**, 347-356 (1994).
- [20] W.Y. PAN, S. SUN and B.A. TUTTLE, *Electromechanical and dielectric instability induced by electric field cycling in ferroelectric ceramic actuators*, *Smart Mater. Struct.*, **1**, 286-293 (1992).
- [21] D.L. POLLA and L.F. FRANCIS, *Ferroelectric thin films in microelectromechanical systems applications*, *MRS Bulletin*, **21**, 7, 59-65 (1996).

- [22] Y. XU, *Ferroelectric materials and their applications*, North-Holland, New York 1991, pp. 206–215.
- [23] R. BRUCHHAUS, H. HUBER, D. PITZER and W. WERSING, *Deposition of ferroelectric PZT thin films by planar multi-target sputtering*, *Ferroelectrics*, **127**, 137–142 (1992).
- [24] O. AUCIELLO, A.I. KINGON and S.B. KRUPANIDHI, *Sputter synthesis of ferroelectric films and heterostructures*, *MRS Bulletin*, **21**, 6, 25–30 (1996).
- [25] Z. SUROWIAK, D. CZEKAJ, A.A. BAKIROV and V.P. DUDKEVICH, *Chemical composition and structure of thin PZT-type ferroelectric films* [in Polish], *Archiwum nauki o materiałach*, **16**, 1, 75–104 (1995).
- [26] Z. SUROWIAK, D. CZEKAJ, A.M. MARGOLIN, E.V. SVIRIDOV, V.A. ALESHIN and V.P. DUDKEVICH, *The structure and the piezoelectric properties of thin $\text{Pb}(\text{Zr}_{0.53}\text{Ti}_{0.45}\text{W}_{0.01}\text{Cd}_{0.01})\text{O}_3$ films*, *Thin Solid Films*, **214**, 78–83 (1992).
- [27] Z. SUROWIAK, D. CZEKAJ, A.A. BAKIROV, E.V. SVIRIDOV and V.P. DUDKEVICH, *The structure and dielectric properties of thin PZT-type ferroelectric films with a diffuse phase transition*, *Integrated Ferroelectrics*, **8**, 267–282 (1995).
- [28] B. JAFFE, W.R. COOK and H. JAFFE, *Piezoelectric ceramics*, Academic Press, London 1971, 137–183.